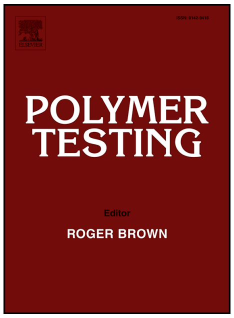

Correlation of molecular parameters, strain hardening modulus and cyclic fatigue test performances of polyethylene materials for pressure pipe applications

Suleyman Deveci, Dongyu Fang

PII: S0142-9418(17)30027-2
DOI: 10.1016/j.polymertesting.2017.07.007
Reference: POTE 5087

To appear in: *Polymer Testing*

Received Date: 9 January 2017
Revised Date: 26 April 2017
Accepted Date: 10 July 2017

Please cite this article as: S. Deveci, D. Fang, Correlation of molecular parameters, strain hardening modulus and cyclic fatigue test performances of polyethylene materials for pressure pipe applications, *Polymer Testing* (2017), doi: 10.1016/j.polymertesting.2017.07.007.

This is a PDF file of an unedited manuscript that has been accepted for publication. As a service to our customers we are providing this early version of the manuscript. The manuscript will undergo copyediting, typesetting, and review of the resulting proof before it is published in its final form. Please note that during the production process errors may be discovered which could affect the content, and all legal disclaimers that apply to the journal pertain.

Correlation of Molecular Parameters, Strain Hardening Modulus and Cyclic Fatigue Test Performances of Polyethylene Materials for Pressure Pipe Applications

Suleyman Deveci[a*], Dongyu Fang[b]

[a]Borouge Innovation Centre, PO 6951, Abu Dhabi, United Arab Emirates

[b]Borouge Co. Ltd., PO 201203, Shanghai, People's Republic of China

*Corresponding Author, e-mail: suleyman.deveci@borouge.com

ABSTRACT

Currently, several testing methods are under development to understand the resistance of polyethylene pipe materials to slow crack growth over comparably short time periods without using aggressive chemicals to accelerate the time to brittle failure. Strain hardening and crack round bar tests have recently been developed and published as ISO testing methods. However, a better understanding of these testing methods is still required with respect to the molecular parameters of the materials. Comparative studies with existing slow crack growth testing methods such as the notched pipe test are of significant interest to the industry. This study discusses correlations of molecular weight, molecular weight distribution, short chain branching and rheological properties of different polyethylene materials with their slow rack growth resistances obtained from the strain hardening and crack round bar tests and their correlations with notched pipe tests.

KEYWORDS: Polyethylene pipes; slow crack growth; notched pipe test; cracked round bar; strain hardening modulus

INTRODUCTION

An increase in the world’s population has created a need for enormous amounts of water to be transported from water sources to communities. This has motivated the technological development of polyethylene materials with improved hydrostatic pressure resistances and with good resistances to slow crack growth. In this context, polyethylene has a good track record over its many years of use for pressurized water and gas transportation networks. High-density, high-molecular-weight polyethylene materials, known as PE80 and PE100 according to ISO 12162, have served the market successfully for many years for standard applications. The performance requirements of these materials with regards to hydrostatic pressure and slow crack growth (SCG) resistance are defined in application-related product specifications. One of several SCG testing methods, the notched pipe test (NPT) [1], developed by Allwood and Beach [2], is defined as a standard testing method to evaluate the SCG performance of PE80 and PE100 materials in ISO product standards [3,4]. In this test, a plastic pipe with four axial predefined notches around its circumference is subjected to hydrostatic pressure in a water bath at a controlled temperature of 80 °C. At the time when NPT was developed, a good PE100 material reached brittle failure at 4.6 MPa after 300–1000 h.

Meanwhile, new trenchless installation techniques, such as horizontal directional drilling [5] and pipe bursting [6] have created a demand for new polyethylene materials with much higher slow crack growth resistances. In response, recent developments in polyethylene production, such as selective incorporation of a 1-hexene co-monomer and bi-modality, have increased the material’s resistance to SCG significantly to successfully meet the new trenchless application requirements. Today, although there is no standardization yet, these materials are known as PE100RC (resistant to crack) type polyethylene in the market [7]. However, despite the use of the surface notch technique for SCG acceleration, current standard testing methods for evaluating the resistance to SCG of PE80- and PE100-type polyethylene materials, such as the NPT, full notched creep test (FNCT) [8] and Pennsylvania notched test (PENT) [9], take a long time to reach brittle failure under standard testing conditions for PE100RC-type materials, in most cases more than 10000 h.

Due to the above-mentioned facts, many researchers have strived to develop new testing methods with higher SCG acceleration that give an idea of the SCG resistance of a pipe material in a shorter time and preferably without using surfactants.

SCG is a time-dependent brittle-type failure that polyethylene pipes show when under low stress levels [10]. The polyethylene's molecular weight (and its distribution), crystallinity, co-monomer type, concentration (and its distribution) [11,12], tie molecules and entanglement density are parameters that are known to affect the SCG of polyethylene. The concept of the strain hardening modulus (Gp) proposed by Haward [13] is based on the entanglement density of a polymer structure. For modern polyethylene materials in particular, Kuralec and co-workers [14] have successfully determined that the strain hardening modulus is a measure of the slow crack growth resistance of polyethylene materials; such a test has become known as the strain hardening (SH) test.

In parallel, Nishimura and Narisawa applied fatigue tests to medium density pipes (cylindrical specimens taken from pipe samples) [15]. Years later, following this work, Pinter and co-authors [16] applied the linear elastic fracture mechanics concept to measure crack initiation and propagation on polyethylene materials. They employed a cylindrical bar with a circumferential notch under a tensile–tensile cyclic test (CRB test); their ranking of polyethylene pipe materials were similar to those determined from the failure times in FNCTs. Subsequently, the method was extended to evaluate the remaining lifetime of polyethylene pipes [17]. Recently, Schoeffl and Lang used the same approach to study the effect of hydrocarbons on the slow crack growth of PE100 materials [18]. In another study, Kratochvilla and co-authors correlated the CRB failure times of polyethylene specimens (directly cut-out from pipe samples) to the failure times of the same pipes in a modified NPT [19].

Recently, SH and CRB testing methods have become ISO testing methods [20,21] for evaluating SCG properties of polyethylene materials. However, there are only a limited number of publications regarding how these new testing methods respond to the material's molecular weight, molecular weight distribution, co-monomer type and viscosity [22–24]. Therefore, these testing methods still require a better understanding with respect to the material's molecular structure, and comparative studies with existing slow crack growth testing methods such as NPT are of great interest to the industry.

In this paper, we report the relationship between the molecular weight, molecular weight distribution, short chain branching and viscosity of PE100- and PE100RC-type materials along with their SH and CRB test performances and the correlation of those testing results to NPT results.

MATERIALS

Ten different commercial grade polyethylene materials with different molecular weights and two different co-monomer types were used in the study. As noted in Table 1, the first two materials were 1-hexene-based PE100 (A1 and A2, respectively), while materials B1, B2 and B3 were 1-butene-based PE100 materials and C1 to C5 were 1-hexene-based PE100RC materials.

EXPERIMENTAL

The weight average molecular weight (MW) and molecular weight distribution (MWD) of the polyethylene materials were obtained by size exclusion chromatography using a conventional procedure [25]. A high-temperature chromatograph equipped with a four band infrared detector was used to determine the molecular weight distribution. 1,2,4-Trichlorobenzene stabilized with 2,6-di tert butyl-4-methyl-phenol was used as the sample solvent and for the mobile phase. The chromatographic system was operated at 160 °C and at a constant flow rate of 1 mL/min; 200 µL of sample solution was injected per analysis.

The viscosities of the materials were determined via a frequency sweep test at 190 °C on a rotational rheometer with a conventional method [26]; parallel plates with a diameter of 25 mm and a gap of 1.2 mm were used.

Specimens for CRB testing had a diameter of 13.8 mm and a length of 100 mm; they were machined from compression moulded plaques. All specimens were notched to a depth of 1.5 mm with a razor blade. The CRB tests were conducted according to ISO18489. The load was applied following a sinusoidal form with a frequency of *f* = 10 Hz and a loading ratio, *R*= *Fmin/Fmax,* of 0.1 at a test temperature of 23 °C. The maximum and minimum loads were calculated according to Equations 1 and 2, respectively.

$$F_{max} = \frac{D_{ini}^2.\pi.\Delta\sigma}{4-(1-R)} \qquad (1)$$

$$F_{min} = F_{max}.R, \qquad (2)$$

where D_{ini} is the initial ligament diameter and $\Delta\sigma$ is the applied stress range. The actual stress range, $\Delta\sigma_0$, on the test specimens was calculated according to Equation 3:

$$\Delta\sigma_0 = \frac{4.\Delta F}{(D-2a_{ini})^2.\pi}, \tag{3}$$

where $\Delta F = F_{max} - F_{min}$, D is the specimen's diameter and a_{ini} is the notch depth measured at the fracture surface following specimen failure.

For each material, at least four different stress ranges were tested and the number of cycles to failure, *N*f, was recorded. A log–log plot of *N*f vs. Δσ was produced and a linear data fit applied with an accuracy of at least *R*2 = 0.98. CRB test failure times at a Δ*σ* of 13 MPa were then calculated for each material based on individual failure plots and used for further comparison.

The SH modulus was determined according to ISO18488 by using ~300 µm thick films. These films were prepared via compression moulding at 180 °C and at a pressure of 5 MPa; they were then cooled down to room temperature at a cooling rate of 15 °C/min. Sheets were annealed at 120 °C for an hour in order to remove residual stresses. The tensile tests on these film samples were conducted at 80 °C with a test speed of 20 mm/min. A non-contact extensometer was used for the strain measurements. The strain hardening modulus, Gp, was calculated using Equation 4, using a linear fit to determine the ratios (λ) (which were between 8 and 12) for the experimentally obtained true stress versus draw ratio curves.

$$\sigma_{true} = Y + Gp\left(\lambda^2 - \frac{1}{\lambda}\right), \tag{4}$$

where

$\sigma_{true} = \lambda\frac{F}{A}$ and $\lambda = 1 + \frac{\Delta l}{l_0}$, where l_0 is the initial gauge length and Δl is the displacement.

NPTs were performed on pipes with an outer diameter of 110 mm and a wall thickness of 10 mm. The tests were performed at 80 °C using 9.2 bar internal pressure until each pipe failed.

RESULTS AND DISCUSSION

Figure 1 shows typical tensile stress–strain curves (engineering stress, σ_{eng}, vs. engineering strain and true stress, σ_{true}, vs. $\lambda^2 - \frac{1}{\lambda}$) at 80 °C. A linear fit to Equation 4 of λ between 8 and 12 is also shown in red.

A closer look at the strain hardening region of the individual curves is shown in Figure 2. A clear distinction between the PE100- (A and B materials) and PE100RC- (C materials) type materials can be observed. All C materials have a steeper slope than the A and B materials.

Figure 3 shows the number of cycles to slow crack growth failure at different stress ranges for each material. All samples showed a good linear fit in log–log graphs. However, the plots are not parallel to each other, making it difficult to rank the various materials for different stress levels. The A materials showed the shortest time to failure, whereas the C materials showed the longest. The results for B materials were somewhere in between; however, an overlap between the B2 and C3 materials is evident.

The SH modulus versus the weight average molecular weight of the materials is given in Figure 4 (bottom). In general, increasing the molecular weight increased the strain hardening modulus for each type of co-monomer material. A similar finding was reported by Haward [27] for high-density polyethylene materials with different molecular weights but similar molecular weight distributions. A good linear correlation between the MW and SH modulus of 1-butene- and 1-hexene-based materials could be established individually; however, the same correlation could not be observed when both the 1-butene- and 1-hexene-based materials were considered together. That is, the 1-hexene co-monomer-type polyethylene materials (A materials, PE100) showed similar or better strain hardening moduli compared to 1-butene-based materials (B materials, PE100) even at lower molecular weights. For similar molecular weights, polyethylene materials with 1-hexene co-monomers (C materials, PE100RC) clearly showed higher strain hardening performances than ones with 1-butene co-monomers (B materials). These findings show that the SH modulus is very sensitive to the co-monomer type and can be a good measure for differentiating 1-butene and 1-hexene based materials that have similar molecular weights.

The relationship between the MW and CRB testing performance of the polyethylene materials is shown in Figure 4 (top). Unlike for SH, a good linear correlation was found between these two parameters for all materials tested, regardless of the type of co-monomer. It is interesting to note that CRB testing is not as sensitive to the type of co-monomer of the materials as the SH test, but both tests are sensitive to the molecular weight of the materials. Having said that, for materials with similar molecular weights (C1, C3, C5 and B3), the CRB tests showed an overlapping performance for both the 1-butene- (PE100) and 1-hexene-based (PE100RC) polyethylenes at a test temperature of 23 °C, whereas the SH test showed a clear distinction between the same materials that overlapped in the CRB tests.

It is shown in Figure 5 that increasing bimodality helps to improve both the SH modulus and CRB performance of polyethylene materials; however, due to other effects such as the MW and co-monomer type the correlation factors tend to be lower. It is also important to note that the effect of the co-monomer type on the SH test is no longer apparent.

Figure 6 shows the relationship between the viscosity (at low shear rates) and the SH modulus and CRB performance of the tested materials. A good statistical correlation is established between the viscosity and the SH modulus of 1-hexene based materials (A and C); however, 1-

butene based materials do not fit this correlation. Similar to the effect of the molecular weight, it is shown that the influence of the co-monomer type is more dominant than the effect of the viscosity on SH. Although having a much higher viscosity, polyethylene materials with 1-butene co-monomers (B) showed a similar or slightly lower SH modulus than the ones with 1-hexene co-monomers (A). In the higher viscosity range, the 1-hexene-based materials (C) showed better strain hardening than the 1-butene-based materials (B).

The relationship between the viscosity and the CRB test performance of polyethylene materials is also given in Figure 6. There is a good agreement with the effect of the MW on CRB, where there is a good linear correlation between the viscosity and the CRB test performance of the polyethylene materials regardless of the type of co-monomer of the polymer.

The NPT vs. SH and CRB results are given in Figure 7. It shows a good statistical correlation between the NPT and SH test and covers both 1-butene and 1-hexene based materials. CRB also shows a good correlation with NPT for 1-hexene-based materials; however, 1-butene-based materials are not covered by this correlation.

Figure 8 shows short the branching content vs. SH and CRB performance of the materials. Although it is not a definitive correlation, increasing the branching content is seen to increase the SH performance of the materials. No correlation was found between the short chain branching and CRB performance of the materials.

Figure 9 shows the SH vs. CRB results. A linear correlation between the SH modulus and CRB performance of the tested materials was found only for 1-hexene based materials (A and C materials), but according to available test data, no overall statistical relationship could be established that covers both 1-butene and 1-hexene based materials.

CONCLUSIONS

In this study, ten different polyethylene materials were analysed to understand the relationship between their molecular weight, molecular weight distribution, short chain branching and viscosities versus their resistance to slow crack growth behaviour obtained from SH, CRB and NPT tests.

We found that both the SH and CRB test performances of materials improved with increased molecular weight, molecular weight distribution, chain branching content and viscosity regardless of the type of co-monomer used. However, for materials with a similar molecular weight, the effect of the type of co-monomer on slow crack growth resistance was better captured in the SH test results. Therefore, the differentiation of 1-butene-based PE100 and 1-hexene-based PE100RC materials can be readily achieved with SH tests.

A good linear correlation between CRB tests and the MW of the materials was observed for all tested samples. However, some overlapping regions were also observed for some of the materials with similar molecular weights but with different co-monomer types. Similar observations were found between the viscosities and the CRB performance of the tested materials.

Furthermore, a very good statistical correlation between the NPT and SH modulus was observed, at least for the materials tested within this study. Although a good statistical correlation between the CRB and NPT performance of 1-hexene- and 1-butene-based materials could be established individually, an overall correlation covering all tested materials was not found. It was also found that 1-hexene-based materials showed a good statistical correlation between SH and CRB tests.

We believe that CRB testing at 80 °C (the same temperature as used for NPT and SH tests) may improve the correlation between the CRB and NPT results. Furthermore, we propose that a combination of SH and CRB test results provide important information about polyethylene materials such that one may be able to confidently predict the long-term performance of polyethylene using such short-term tests.

REFERENCES

[1] ISO 13479:2009 Polyolefin pipes for the conveyance of fluids — Determination of resistance to crack propagation — Test method for slow crack growth on notched pipes, (2012).

[2] W.J. Allwood, S.H. Beach, S.H. Beech, The development of the “notched pipe test” for the assessment of the slow crack growth resistance of polyethylene pipe, Constr. Build. Mater. 7 (1993) 157–162.

[3] ISO 4427-2:2007 Plastics piping systems -- Polyethylene (PE) pipes and fittings for water supply -- Part 2: Pipes, (n.d.).

[4] ISO 4437-2:2014 Plastics piping systems for the supply of gaseous fuels - Polyethylene (PE) -- Part 2: Pipes, (n.d.).

[5] M.A. Polak, Analysis of polyethylene pipe behaviour in horizontal directional drilling field tests, Can. J. Civ. Eng. 32 (2005) 665–677. doi:10.1139/l05-013.

[6] J. Lueke, S. Ariaratnam, Rehabilitation of Underground Infrastructure Utilizing Trenchless Pipe Replacement, Pract. Period. Struct. Des. Constr. 6 (2001) 25–34. doi:10.1061/(ASCE)1084-0680(2001)6:1(25).

[7] D.W. Andrew Wedgner, Alex Stewart, The Introduction of High Stress Crack Resistant PE100 and its use in several demanding projects in Asia and the Middle East, in: Proc. Plast. Pipe XVI, Barcelona, 2012.

[8] ISO 16770:2004 Plastics -- Determination of environmental stress cracking (ESC) of polyethylene -- Full-notch creep test (FNCT), (n.d.).

[9] ASTM F1473 - 16 Standard Test Method for Notch Tensile Test to Measure the Resistance to Slow Crack Growth of Polyethylene Pipes and Resins, (n.d.).

[10] X. Lu, N. Brown, X. Lu, A fundamental theory for slow crack growth in polyethylene, Polymer (Guildf). 36 (1995) 543–548.

[11] R.K. Krishnaswamy, Q. Yang, L. Fernandez-ballester, J.A. Kornfield, Effect of the distribution of short-chain branches on crystallization kinetics and mechanical properties of high-density polyethylene, Macromolecules. 41 (2008) 1693–1704.

[12] B. Na, R. Lv, W. Xu, P. Yu, K. Wang, Q. Fu, Inverse temperature dependence of strain hardening in ultrahigh molecular weight polyethylene: Role of lamellar coupling and entanglement density, J. Phys. Chem. B. 111 (2007) 13206–13210.

[13] R.N. Haward, Strain hardening of thermoplastics, Macromolecules. 26 (1993) 5860–5869.

[14] L. Kurelec, M. Teeuwen, H. Schoffeleers, R. Deblieck, Strain hardening modulus as a measure of environmental stress crack resistance of high density polyethylene, 46 (2005) 6369–6379. doi:10.1016/j.polymer.2005.05.061.

[15] H. Nishimura, I. Narisawa, Fatigue behavior of medium□density polyethylene pipes, Polym. Eng. Sci. 31 (1991) 399–403.

[16] G. Pinter, M. Haager, W. Balika, R.W. Lang, Cyclic crack growth tests with CRB specimens for the evaluation of the long-term performance of PE pipe grades, Polym. Test. 26 (2007) 180–188. doi:http://dx.doi.org/10.1016/j.polymertesting.2006.09.010.

[17] A. Frank, G. Pinter, R.W. Lang, Prediction of the remaining lifetime of polyethylene pipes after up to 30 years in use, Polym. Test. 28 (2009) 737–745. doi:http://dx.doi.org/10.1016/j.polymertesting.2009.06.004.

[18] P.F. Schoeffl, R.W. Lang, Effect of liquid oilfield-related media on slow crack growth behavior in polyethylene pipe grade materials, Int. J. Fatigue. 72 (2015) 90–101. doi:http://dx.doi.org/10.1016/j.ijfatigue.2014.09.016.

[19] T.R. Kratochvilla, A. Frank, G. Pinter, Determination of slow crack growth behaviour of polyethylene pressure pipes with cracked round bar test, Polym. Test. 40 (2014) 299–303. doi:10.1016/j.polymertesting.2014.10.002.

[20] ISO 18488 Polyethylene (PE) materials for piping systems — Determination of Strain Hardening Modulus in relation to slow crack growth — Test method, 2015 (2015).

[21] ISO 18489 Polyethylene (PE) materials for piping systems — Determination of resistance to slow crack growth under cyclic loading — Cracked Round Bar test method, (2015).

[22] R.A.C. Deblieck, D.J.M. Van Beek, K. Remerie, I.M. Ward, Failure mechanisms in polyolefines : The role of crazing, shear yielding and the entanglement network, Polymer (Guildf). 52 (2011) 2979–2990. doi:10.1016/j.polymer.2011.03.055.

[23] A. Redhead, G. Pinter, A. Frank, Analysis of Molecular and Morphological Effects on Slow Crack Growth in Modern PE Pipe Grades by Cyclic Fracture Mechanics Tests, Macromol. Symp. 311 (2012) 41–48. doi:10.1002/masy.201000110.

[24] J. Fawaz, S. Deveci, V. Mittal, Molecular and morphological studies to understand slow crack growth (SCG) of polyethylene, Colloid Polym. Sci. 294 (2016) 1269–1280. doi:10.1007/s00396-016-3888-5.

[25] ASTM D6474 - 12 Standard Test Method for Determining Molecular Weight Distribution and Molecular Weight Averages of Polyolefins by High Temperature Gel Permeation Chromatography, (n.d.).

[26] ISO 6721-10:2015 Plastics -- Determination of dynamic mechanical properties -- Part 10: Complex shear viscosity using a parallel-plate oscillatory rheometer, (n.d.).

[27] R.N. Haward, E. Barn, O. Ditch, U. Kingdom, Strain hardening of high density polyethylene, J. Polym. Sci. Part B Polym. Phys. 45 (2007) 1090–1099. doi:10.1002/polb.

Figure Captions

Figure 1 : engineering strain and engineering stress curve (black curve with right and top axes), and strain hardening curve (blue curve with bottom and left axes), along with linear fitting line in red.

Figure 2: Strain hardening region of individual curves

Figure 3: Number of cycles till brittle failure vs. applied stress for each material. Red lines represent linear data fitting with min R^2 of 0.98

Figure 4: MW vs. CRB failure cycles at $\Delta\sigma_0$ of 13 MPa (top), and MW vs. SH modulus of materials (bottom). Black lines represent linear data fitting.

Figure 5: MWD vs. CRB failure cycles at $\Delta\sigma_0$ of 13 MPa (top), and MWD vs. SH modulus of materials (bottom). Black lines represent linear data fitting.

Figure 6: Viscosity (ETA at 0.05 rad/s) vs. CRB failure cycles at $\Delta\sigma_0$ of 13 MPa (top), and Viscosity (ETA at 0.05 rad/s) vs. SH modulus of materials (bottom). Black lines represent linear data fitting.

Figure 7: NPT failure times vs. CRB failure cycles at $\Delta\sigma_0$ of 13 MPa (top), and NPT failure times vs. SH modulus of materials (bottom). Black lines represent linear data fitting.

Figure 8: Co-monomer content (C-1000) vs. CRB failure cycles at $\Delta\sigma_0$ of 13 MPa (top), and Co-monomer content (C-1000) vs. SH modulus of materials (bottom). Black line represents linear data fitting. C-1000 values are obtained by H-NMR tests.

Figure 9: SH vs. CRB test performance of materials. Black line represents linear data fitting.

Table 1 Designation of materials, co-monomer type and classification

Designation	Co-Monomer Type	Classification
A1	1-hexene	PE100
A2	1-hexene	PE100
B1	1-butene	PE100
B2	1-butene	PE100
B3	1-butene	PE100
C1	1-hexene	PE100RC
C2	1-hexene	PE100RC
C3	1-hexene	PE100RC
C4	1-hexene	PE100RC
C5	1-hexene	PE100RC

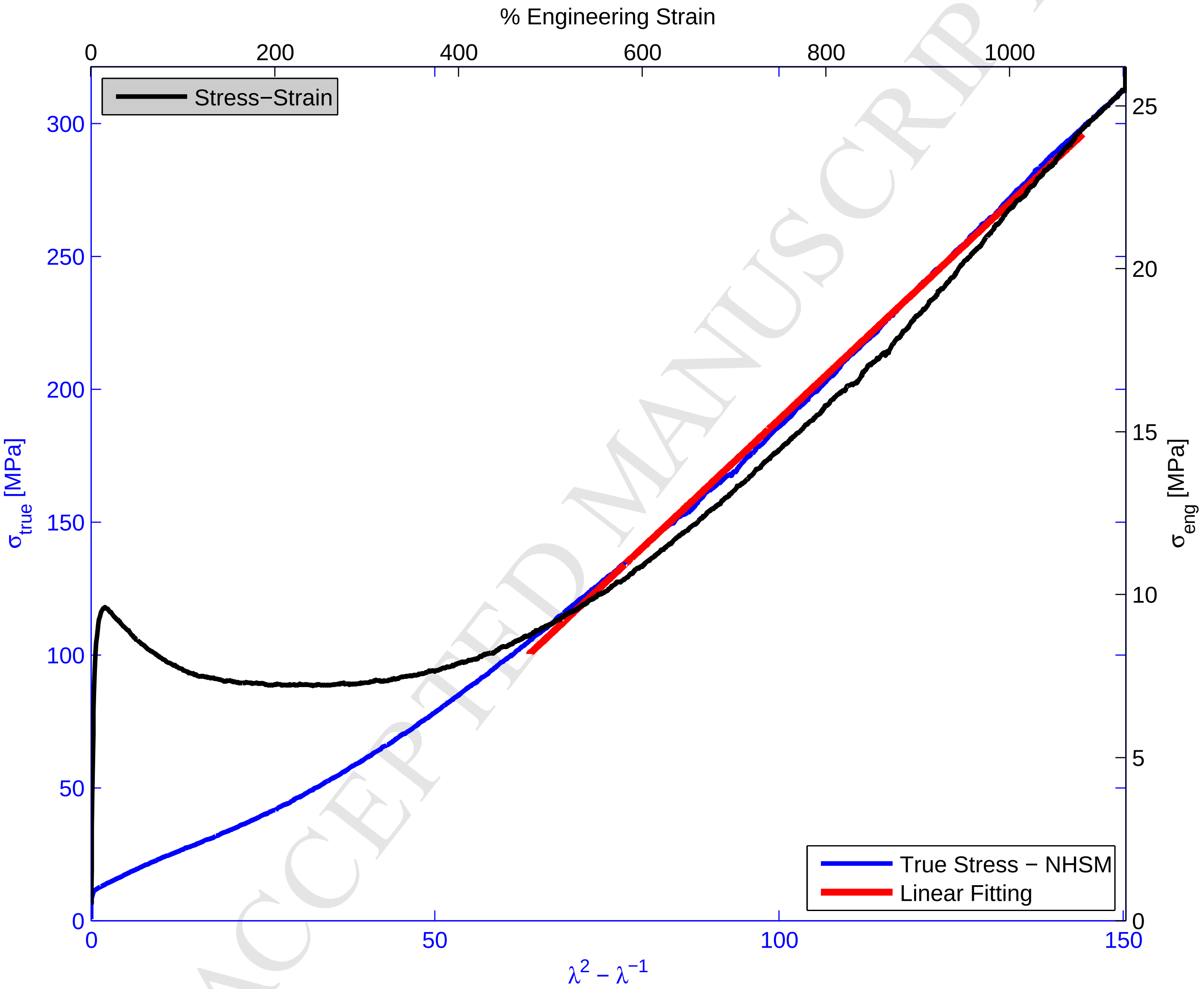
% Engineering Strain
0
200
400
600
800
1000
Stress−Strain
σ_true [MPa]
300
250
200
150
100
50
0
25
20
15
10
5
0
σ_eng [MPa]
True Stress − NHSM
Linear Fitting
0
50
100
150
λ^2 − λ^−1

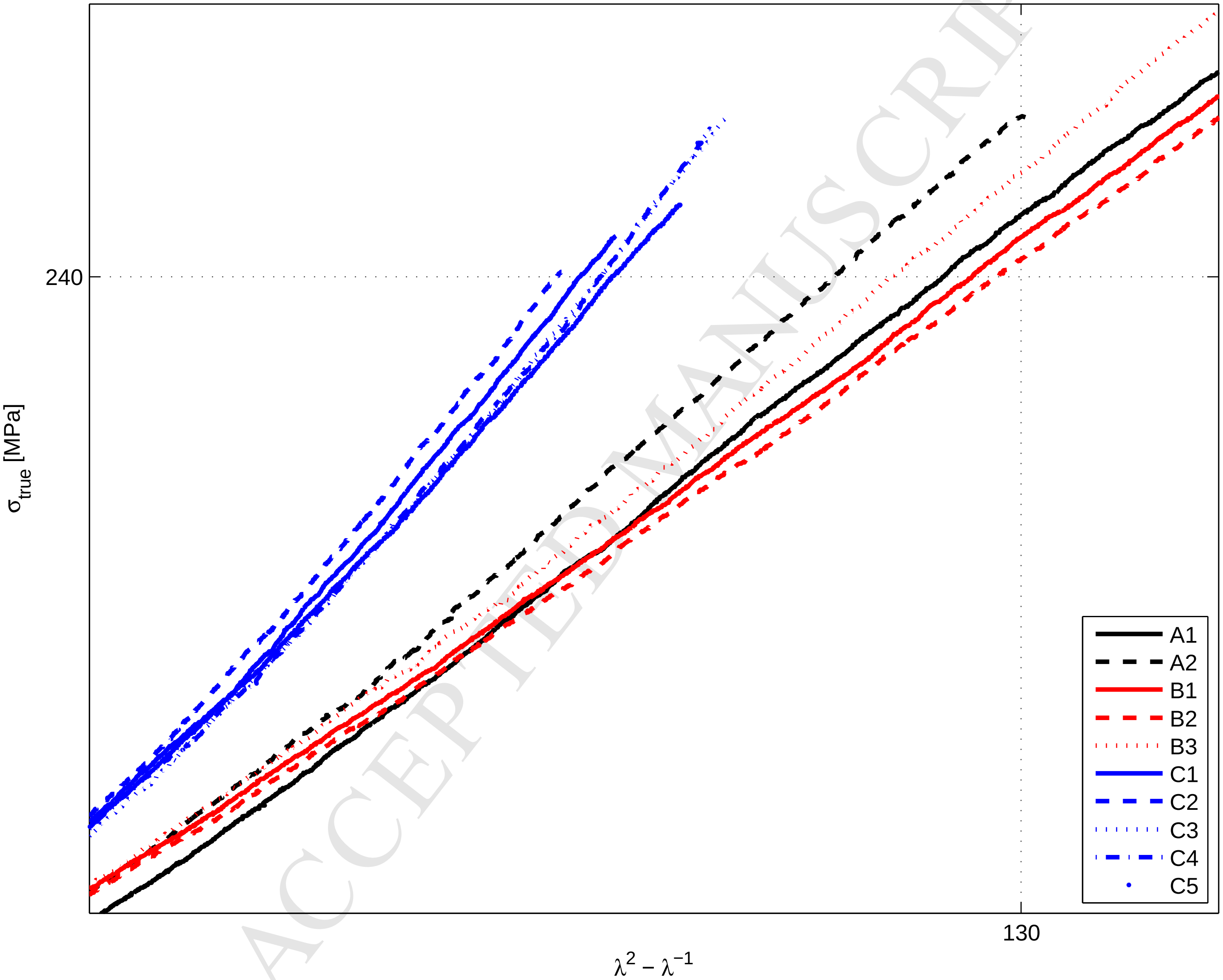
240
130
σ_{true} [MPa]
$\lambda^2 - \lambda^{-1}$
A1
A2
B1
B2
B3
C1
C2
C3
C4
C5

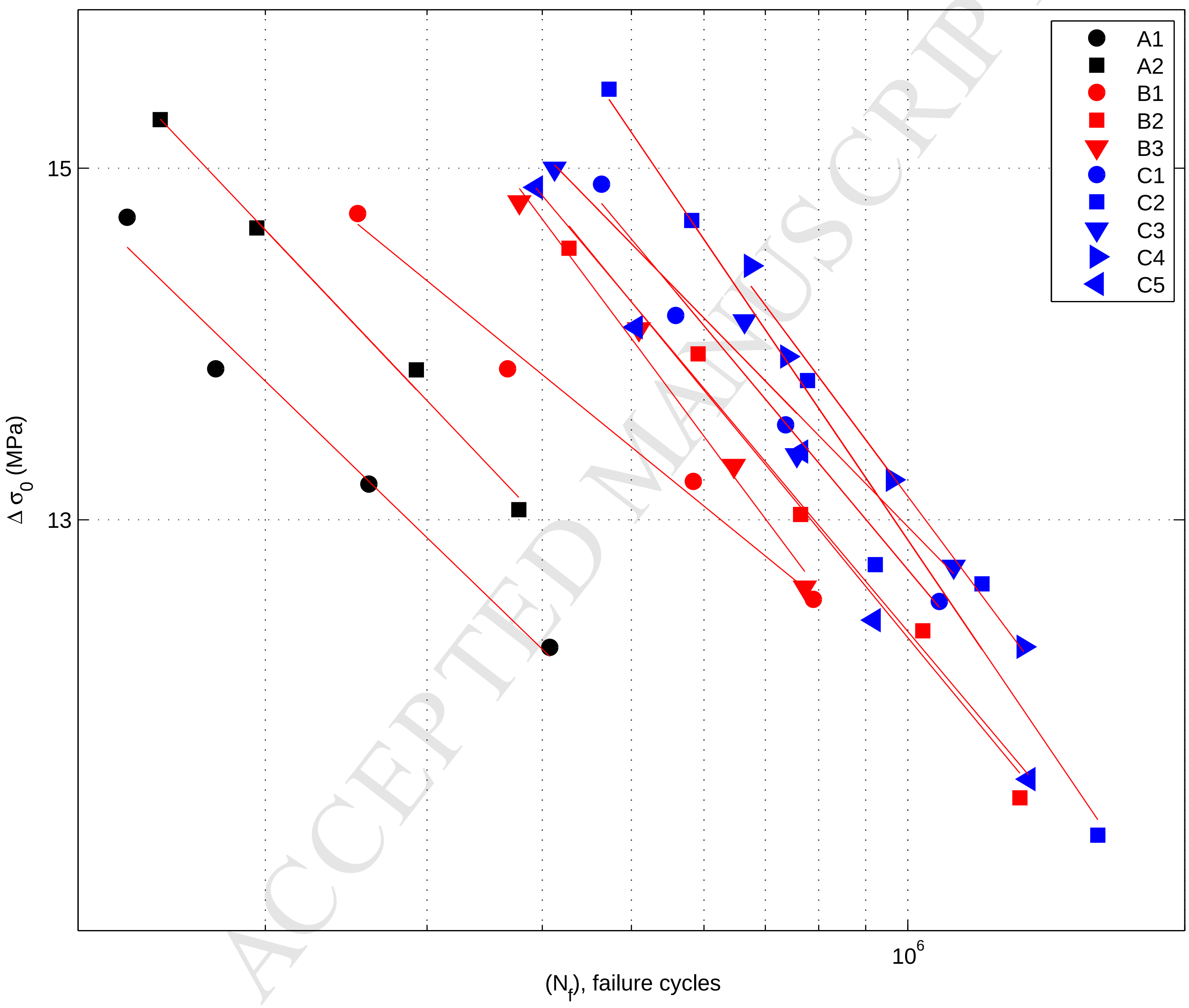
15
13
Δ σ_0 (MPa)
10^6
(N_f), failure cycles
A1
A2
B1
B2
B3
C1
C2
C3
C4
C5

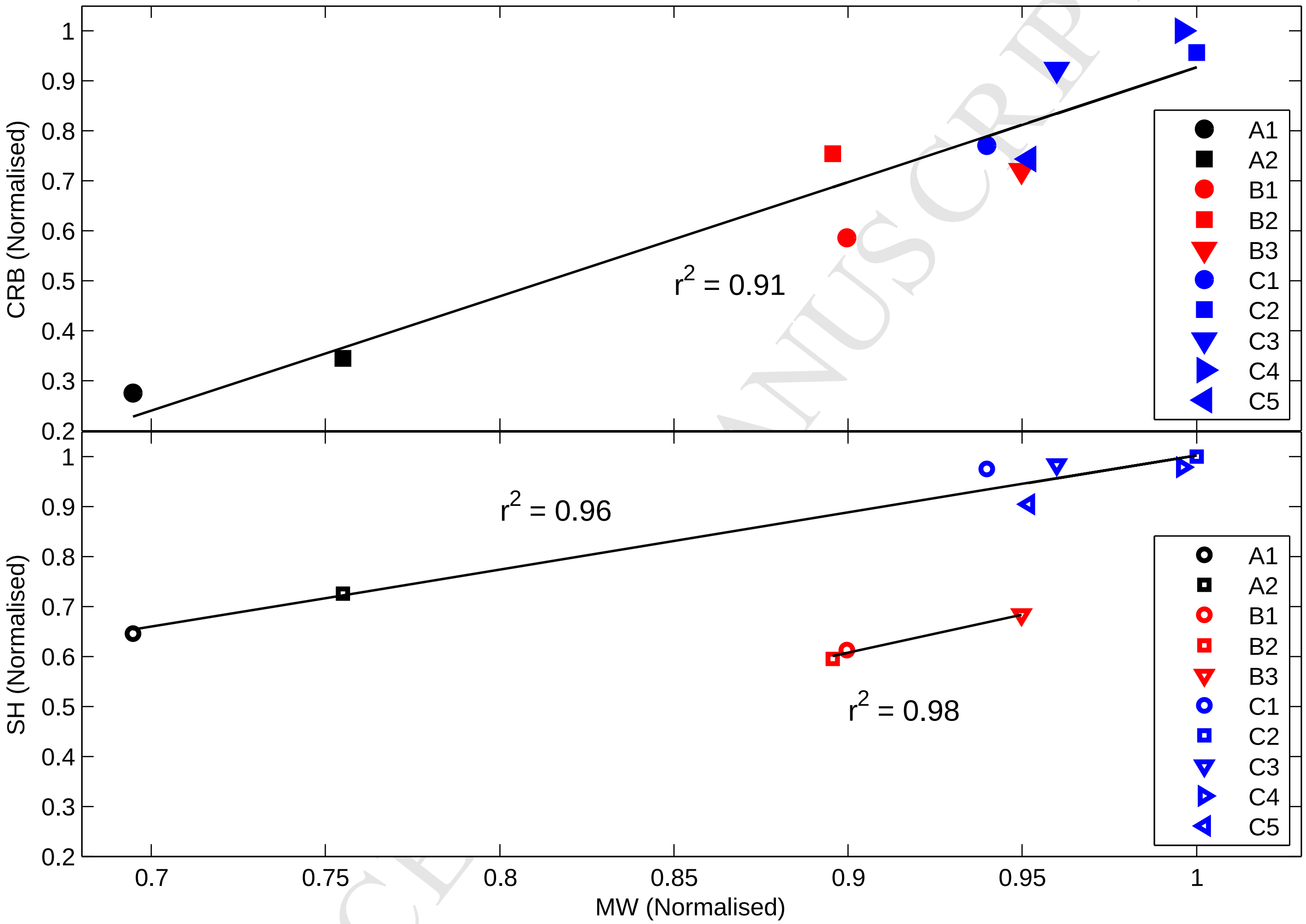
CRB (Normalised)
1
0.9
0.8
0.7
0.6
0.5
0.4
0.3
0.2
r^2 = 0.91
A1
A2
B1
B2
B3
C1
C2
C3
C4
C5
SH (Normalised)
1
0.9
0.8
0.7
0.6
0.5
0.4
0.3
0.2
r^2 = 0.96
r^2 = 0.98
A1
A2
B1
B2
B3
C1
C2
C3
C4
C5
0.7
0.75
0.8
0.85
0.9
0.95
1
MW (Normalised)

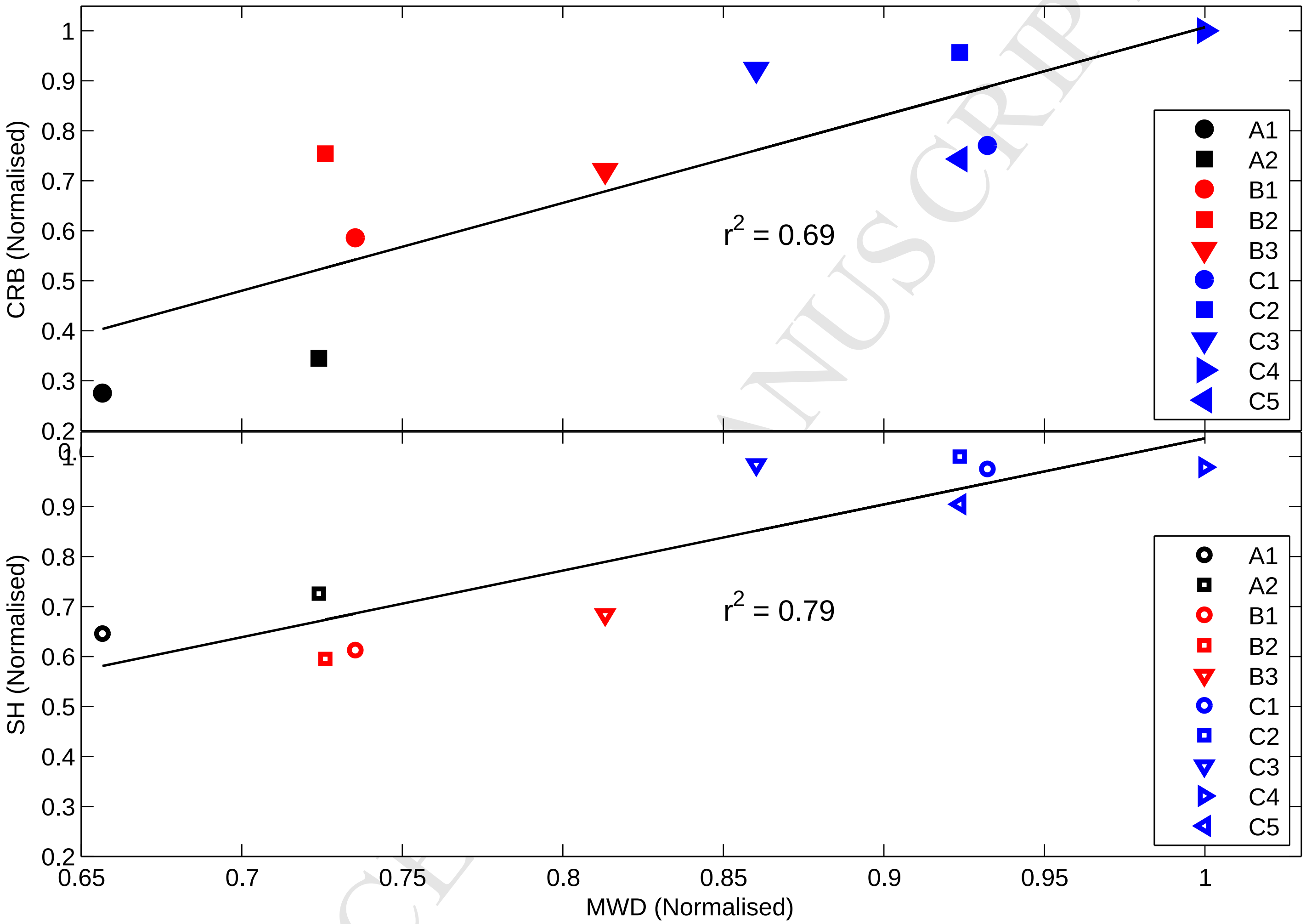
CRB (Normalised)
1
0.9
0.8
0.7
0.6
0.5
0.4
0.3
0.2
r² = 0.69
A1
A2
B1
B2
B3
C1
C2
C3
C4
C5
SH (Normalised)
1
0.9
0.8
0.7
0.6
0.5
0.4
0.3
0.2
r² = 0.79
0.65
0.7
0.75
0.8
0.85
0.9
0.95
1
MWD (Normalised)

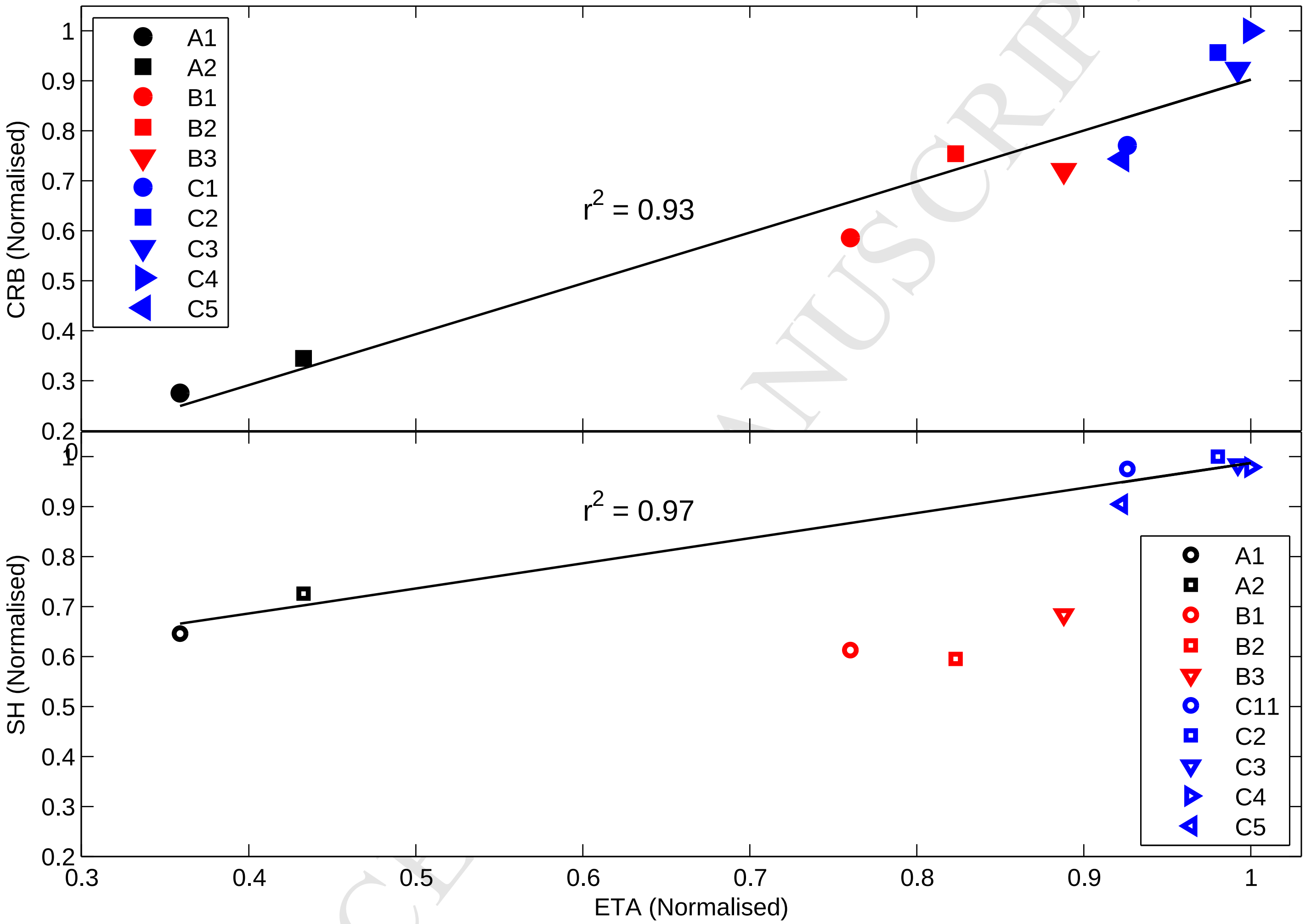

CRB (Normalised)
r^2 = 0.93
SH (Normalised)
r^2 = 0.97
ETA (Normalised)
A1
A2
B1
B2
B3
C1
C11
C2
C3
C4
C5
0.2
0.3
0.4
0.5
0.6
0.7
0.8
0.9
1

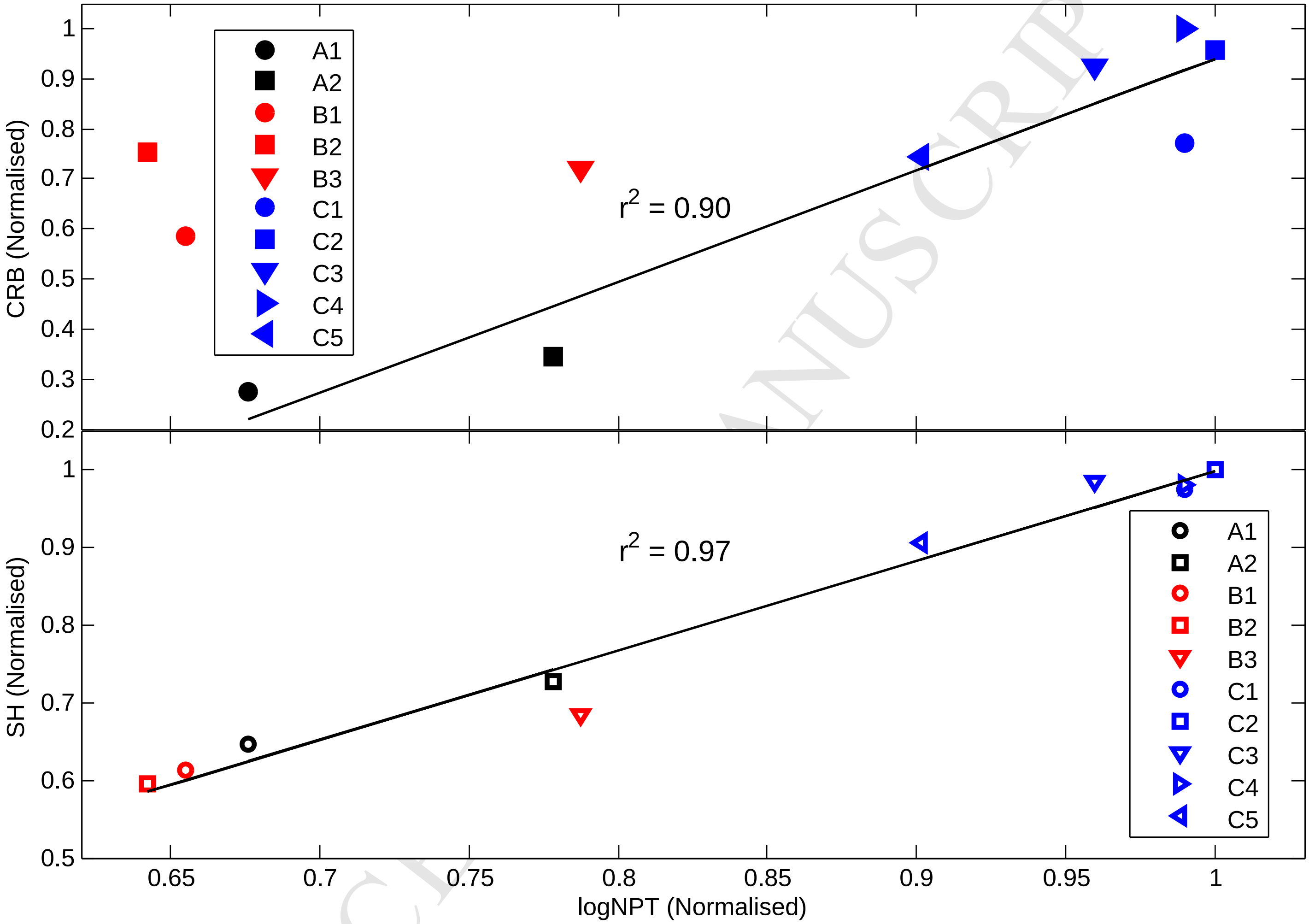
CRB (Normalised)
1
0.9
0.8
0.7
0.6
0.5
0.4
0.3
0.2
A1
A2
B1
B2
B3
C1
C2
C3
C4
C5
r^2 = 0.90
SH (Normalised)
0.5
0.6
0.7
0.8
0.9
1
r^2 = 0.97
0.65
0.7
0.75
0.8
0.85
0.9
0.95
1
logNPT (Normalised)

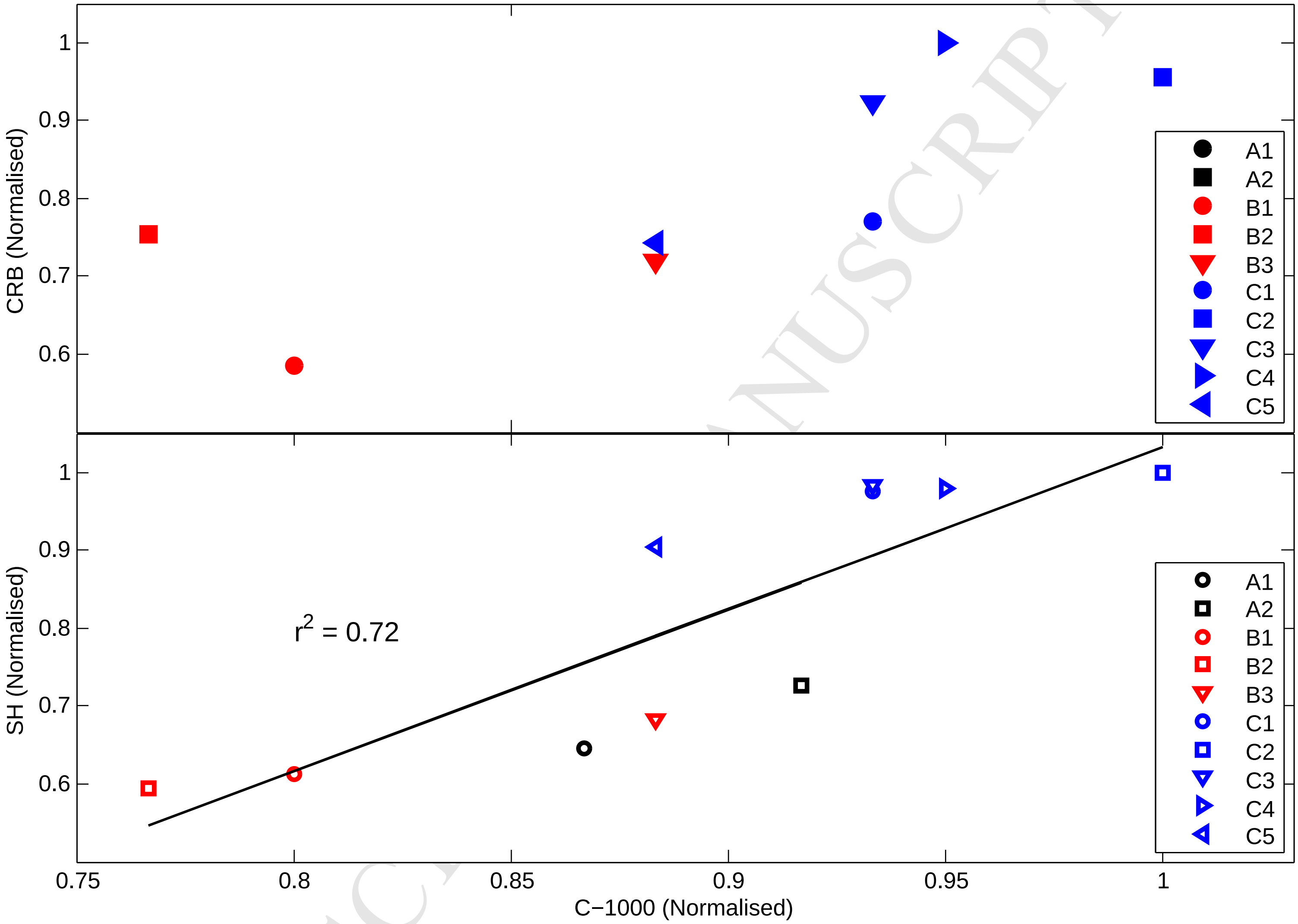
CRB (Normalised)
1
0.9
0.8
0.7
0.6
A1
A2
B1
B2
B3
C1
C2
C3
C4
C5
SH (Normalised)
r^2 = 0.72
1
0.9
0.8
0.7
0.6
0.75
0.8
0.85
0.9
0.95
1
C−1000 (Normalised)

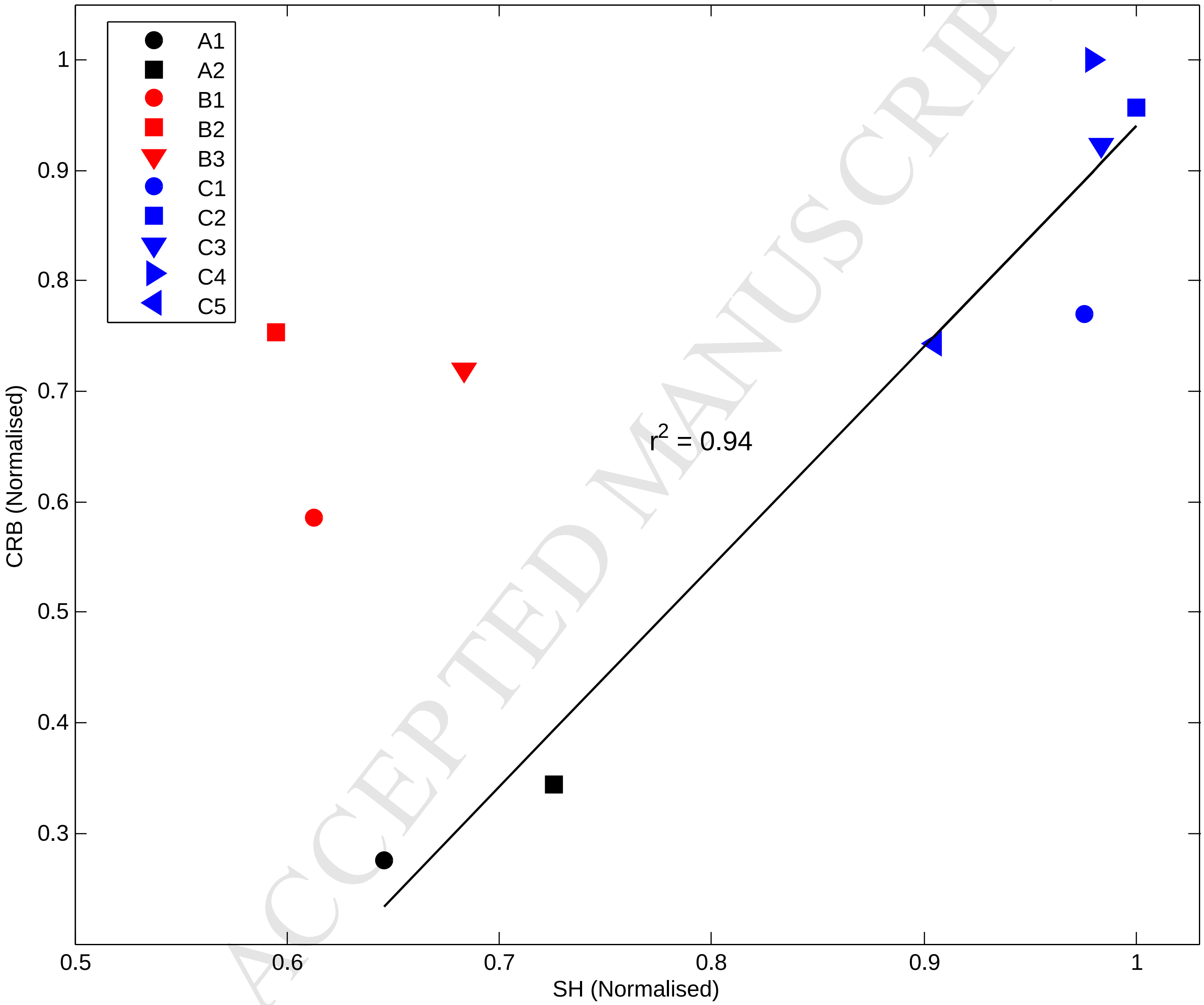
A1
A2
B1
B2
B3
C1
C2
C3
C4
C5
r^2 = 0.94
CRB (Normalised)
SH (Normalised)
1
0.9
0.8
0.7
0.6
0.5
0.4
0.3
0.5
0.6
0.7
0.8
0.9
1